Nucleosynthesis of ^{26}Al in massive stars: New ^{27}Al states above α and neutron emission thresholds

S. Benamara,[1,2] N. de Séréville,[2,*] A. M. Laird,[3] F. Hammache,[2] I. Stefan,[2] P. Roussel,[2] S. Ancelin,[2] M. Assié,[2] A. Coc,[4] I. Deloncle,[4] S. P. Fox,[3] J. Kiener,[4] L. Lefebvre,[2] A. Lefebvre-Schuhl,[4] G. Mavilla,[2] P. Morfouace,[2] Á. M. Sánchez-Benítez,[5,†] L. Perrot,[2] M. Sinha,[6] V. Tatischeff,[4] and M. Vandebrouck[2]

[1]*Laboratoire de Physique et Chimie Quantique, Université Mouloud Mammeri, Tizi-Ouzou, Algeria*

[2]*Institut de Physique Nucléaire d'Orsay, UMR8608, IN2P3-CNRS, Université Paris Sud 11, 91406 Orsay, France*

[3]*Department of Physics, University of York, York YO10 5DD, United Kingdom*

[4]*CSNSM, IN2P3-CNRS et Université Paris Sud 11, 91405 Orsay Campus, France*

[5]*Departamento de Física Aplicada, Universidad de Huelva, E-21071 Huelva, Spain*

[6]*Saha Institute of Nuclear Physics, 1/AF, Bidhannagar, Kolkata 700064, India*

(Received 15 January 2014; revised manuscript received 21 April 2014; published 25 June 2014)

The ^{26}Al radioisotope is of great importance for understanding the chemical and dynamical evolution of our galaxy. Among the possible stellar sources, massive stars are believed to be the main producer of this radioisotope. Understanding ^{26}Al nucleosynthesis in massive stars requires estimates of the thermonuclear reaction rates of the ^{26}Al$(n,p)^{26}$Mg, ^{26}Al$(n,\alpha)^{23}$Na, and ^{23}Na$(\alpha,p)^{26}$Mg reactions. These reaction rates depend on the spectroscopic properties of ^{27}Al states above the neutron and alpha thresholds. In this context, the ^{27}Al$(p,p')^{27}$Al* reaction was studied at 18 MeV using a high-resolution Enge Split-Pole spectrometer. States from the ground state up to excitation energies of ≈14 MeV were populated. While up to the ^{23}Na + α threshold no additional states are observed, we report for the first time 30 new levels above the ^{23}Na + α threshold and more than 30 new states above the ^{26}Al + n threshold for which excitation energies are determined with an uncertainty of 4–5 keV.

DOI: 10.1103/PhysRevC.89.065805 PACS number(s): 25.40.Ep, 26.20.Np, 27.30.+t, 29.30.Aj

I. INTRODUCTION

^{26}Al is a radioisotope produced in a variety of stellar sites [1] such as massive stars (Wolf-Rayet phase and core-collapse supernovae), asymptotic giant branch (AGB) stars, and classical nova outbursts. Its ground state β^+ decays to the first excited state of ^{26}Mg which then deexcites to its ground state, emitting a characteristic γ-ray line at $E_\gamma = 1.809$ MeV.

The γ-ray emission at 1.809 MeV has been observed in our galaxy with many γ-ray detectors on stratospheric balloons and aboard spacecraft [2–4]. These observations provided a confirmation that ongoing nucleosynthetic processes are active in the galaxy since the ^{26}Al half-life ($T_{1/2} = 7.2 \times 10^5$ yr) is very short compared to the time scale of galactic chemical evolution ($\approx 10^{10}$ yr). Subsequently, the first all-sky map of the 1.809 MeV γ-ray line was obtained with the COMPTEL instrument on board the CGRO satellite [5]. This map revealed a diffuse emission along the galactic plane with hot spots associated with massive star regions (e.g., Cygnus and Vela regions). Comparison of the ^{26}Al map with all-sky maps at other wavelengths have shown that the 1.809 MeV γ-ray emission is correlated to tracers of the massive star population [6]. More recently, high spectral resolution measurements of ^{26}Al emission at 1.809 MeV made by the SPI/INTEGRAL instrument further demonstrated that ^{26}Al sources co-rotate with the galaxy, supporting its galaxy-wide origin [7,8].

The first evidence of ^{26}Al in meteorites [9] was observed in calcium-aluminum rich inclusions (CAIs) from the Allende meteorite as an excess of its daughter nuclei (^{26}Mg) with respect to the stable ^{24}Mg isotope. The linear correlation between the ^{26}Mg/^{24}Mg and ^{27}Al/^{24}Mg isotopic ratios yields an initial value of 5.3×10^{-5} for the ^{26}Al/^{27}Al ratio [10]. Since CAIs were among the first solids to condense in the early Solar System, the presence of ^{26}Al demonstrates that this short-lived nucleus was indeed *present* during the very first million years following the gravitational collapse of the proto-sun. Of the many other extinct radioactivities which have been identified, ^{26}Al is the radionucleus for which the initial content is best constrained. Understanding the origin of ^{26}Al can then provide crucial information concerning our Solar System formation. Among the available scenarios, contamination of the proto–Solar System by massive stars is favored [11,12].

Production of ^{26}Al in massive stars occurs at different stages of their evolution, including core hydrogen burning, neon/carbon convective shell burning, as well as explosive neon burning. Calculations of ^{26}Al yields in each burning phase have shown that ^{26}Al is mainly produced by explosive Ne/C burning over most of the initial range between 11 and 120 solar masses [13]. In order to identify the nuclear reactions which most affect ^{26}Al production, post-processing nucleosynthesis calculations have been performed for each burning phase [14]. It was found that only a few reaction rate uncertainties influence the ^{26}Al nucleosynthesis. Particularly important reactions are ^{26}Al$(n,p)^{26}$Mg and ^{26}Al$(n,\alpha)^{23}$Na in the explosive Ne/C burning and the C/Ne shell burning phases as well as the ^{23}Na$(\alpha,p)^{26}$Mg reaction in the C/Ne shell burning phase. In their work, Iliadis *et al.* [14] indicated that the aforementioned reactions "should be prime targets for future measurements." Note that the ^{23}Na$(\alpha,p)^{26}$Mg reaction also plays an important role in type Ia supernovae nucleosynthesis [15,16].

*deserevi@ipno.in2p3.fr

†Present address: Centro de Física Nuclear da Universidade de Lisboa, 1649-003 Lisboa, Portugal.

For typical temperatures (≈2.3 GK) achieved during the explosive burning phase, the ^{27}Al states populated by the ^{26}Al$(n,p)^{26}$Mg and ^{26}Al$(n,\alpha)^{23}$Na reactions are within about 500 keV above the ^{26}Al + n threshold (S_n = 13.057 MeV). These levels, being at higher energies than the ^{26}Mg + p and ^{23}Na + α thresholds (S_p = 8.271 MeV, S_α = 10.092 MeV), will decay, emitting protons and alpha particles. Due to the radioactive nature of ^{26}Al and the difficulty of producing large surface density targets, the first experimental determination of the ^{26}Al$(n,p)^{26}$Mg and ^{26}Al$(n,\alpha)^{23}$Na reaction rates was based on the study of the time-reverse reactions ^{26}Mg$(p,n)^{26}$Al and ^{23}Na$(\alpha,n)^{26}$Al using the principle of detailed balance [17]. However, this method only provides the branching to the ground state of ^{26}Mg and ^{23}Na and thus can underestimate the reaction rate. This is the case for the ^{26}Al$(n,p)^{26}$Mg reaction, which is dominated by the (n,p_1) channel, due to the respective spins and parities of the ground (0^+) and first (2^+) excited states in ^{26}Mg. With the advent of ^{26}Al targets, direct measurements have been performed [18–20] and a few narrow resonances have been observed within 100 keV above the ^{26}Al + n threshold [19,20]. The ^{26}Al$(n,p)^{26}$Mg reaction cross section was also measured for neutron energies between 270 and 350 keV [18]. Only two experimental reaction rates for ^{26}Al$(n,p)^{26}$Mg are available so far [18,19], and even if they cover distinct temperature regions, they appear to be inconsistent (see Fig. 1 from Oginni *et al.* [21]). A similiar situation exists for the ^{26}Al$(n,\alpha)^{23}$Na reaction rate where the two existing experimental determinations [19,20] are inconsistent by more than a factor of 2, and only cover temperatures lower than those operating in the explosive Ne/C phase (see Fig. 2 from Oginni *et al.* [21]). Given this situation, the reaction rates used in stellar evolution calculations, for the temperatures of interest, are based on the Hauser-Feshbach statistical approach [22]. The expected level density at excitation energies of ≈13 MeV in ^{27}Al should be high enough to justify the use of the statistical model. However, since the ^{26}Al ground state has $J^\pi = 5^+$, ^{27}Al states which are likely to have the most important effect in the reaction rate have high spins such as $9/2^+$ and $11/2^+$ or $7/2^-$ to $13/2^-$ for s- or p-wave neutron capture, respectively. Only a fraction of the states will have such high spin and this could question the use of Hauser-Feshbach calculations in this case. This is supported by the small number of resonances observed in the direct ^{26}Al + n experiments [19,20].

For typical temperatures (≈1.25 GK) achieved during the C/Ne shell burning phase, the Gamow peak for the ^{23}Na$(\alpha,p)^{26}$Mg reaction covers a center-of-mass energy range $E_{\text{c.m.}}$ = 1.2–2.2 MeV. The only direct measurement of this reaction [23] does not cover the lower energy part of the Gamow peak (e.g., $E_{\text{c.m.}} > 1.96$ MeV). Absolute resonance strengths for 39 new resonances are reported with respect to previous experimental work [24]. However, the results of Whitmire *et al.* [23] suffer from several experimental problems, including possible change of the NaCl target stoichiometry affecting an accurate determination of the resonance strengths, as well as a large uncertainty in the determination of the resonance energies (about 10 keV). As a result of these issues the ^{23}Na$(\alpha,p)^{26}$Mg reaction rate used in stellar evolution calculations is also based on the Hauser-Feshbach model [22].

Constraining the ^{26}Al$(n,p)^{26}$Mg, ^{26}Al$(n,\alpha)^{23}$Na, and ^{23}Na$(\alpha,p)^{26}$Mg reaction rates in massive stars during the explosive Ne/C burning and shell C/Ne burning is very important to better understand the nucleosynthesis of the ^{26}Al radioisotope. In this context knowledge of the structure of ^{27}Al within around 500 keV above the ^{26}Al + n threshold and above the ^{23}Na + α threshold is of clear importance. Here we report on a high-precision study of inelastic proton scattering off ^{27}Al to populate, and determine the energies of, relevant states in ^{27}Al. This reaction was chosen since inelastic proton scattering is known to be unselective [25,26] and thus allow a comparison with all known states.

II. EXPERIMENT

The ^{27}Al$(p,p')^{27}$Al* reaction was studied at the Tandem-Alto facility in Orsay, France. A proton beam of about 300 nA was produced by the duoplasmatron ion source and accelerated by the 15 MV Tandem to an energy of 18 MeV. The beam was transported to the target located at the object focal point of an Enge Split-Pole magnetic spectrometer [27]. A self-supporting ^{27}Al target with a thickness of 89 ± 8 μg/cm^2 was used. Natural carbon (80 μg/cm^2) and mylar ($C_{10}H_8O_4$, 203 μg/cm^2) targets were also used to characterize the background due to reactions on carbon and oxygen present as contaminants in the aluminum target. When using the mylar target the beam intensity was reduced to about 20 nA in order to avoid target deterioration. All target thicknesses were determined by measuring the energy loss of alpha particles emitted by a ^{241}Am source. Light reaction products entered the Split-Pole spectrometer through a rectangular aperture covering a 1.2 msr solid angle, and were momentum analyzed and focused on the focal-plane detection system [28]. This system consisted of a 50 cm long position sensitive gas chamber, a ΔE proportional gas counter, and a plastic scintillator measuring the residual energy. Particle identification was achieved through energy loss versus position measurement and the inelastic protons were readily separated from the deuterons produced by the ^{27}Al$(p,d)^{26}$Al reaction as shown in Fig. 1.

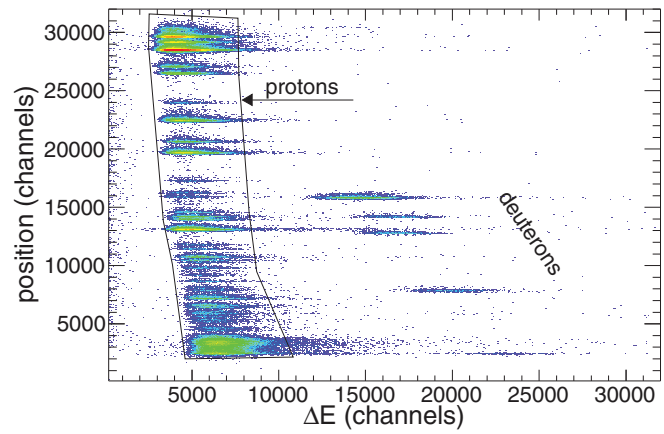

FIG. 1. (Color online) Particle identification spectrum (position versus energy loss) obtained with the focal-plane detector. Protons and deuterons are easily distinguished. The proton selection cut is represented.

After selection, proton spectra of the focal-plane position were then obtained. Measurements were performed at spectrometer angles of 10°, 40°, and 45°. At 10° and 40° a series of four overlapping spectra covering ^{27}Al excitation energies from the ground state up to about 14 MeV were obtained by changing the magnetic field four times. The overlap in each case was about one third of the focal-plane length which allowed the stability of experimental conditions to be checked. At 45° only two exposures were measured corresponding to the highest excitation energy range (9.4 to 14 MeV). The position of the focal-plane detector was moved backward and adjusted to cancel the kinematic broadening so that resolutions (FWHM) in the laboratory frame of 22 and 12 keV were obtained for excitation energies of 4.5 and 13 MeV, respectively.

III. DATA ANALYSIS AND DISCUSSIONS

A. Calibration and peak identification

A careful focal-plane detector calibration was performed using low-excitation energy exposure (see Fig. 2) where well known isolated states are strongly populated. Important parameters for the calibration are accurate values of the beam energy ($E_{\rm beam}$) and the spectrometer angle (θ_{SP}). These parameters were determined by an iterative procedure using the ^{27}Al$(p,p')^{27}$Al* reaction in addition to the ^{12}C$(p,p')^{12}$C$_{4.44}$, ^{16}O$(p,p')^{16}$O$_{6.13}$, and ^{27}Al$(p,d)^{26}$Al (ground state and first three excited states) reactions which show different kinematic dependencies to the beam energy and detection angle. In a first step, eleven ^{27}Al states [843.76(9), 1014.56(9), 2212.01(10), 2734.9(7), 4410.2(4), 4510.3(4), 4580.0(8), 5155.6(8), 5248.0(6), 5960.3(7), and 6651.3(7) keV] across the whole focal plane were used to obtain a relation between the radius of curvature ρ and the focal-plane position. The calibration was then obtained by fitting the previous relation with a one-degree polynomial function. In a second step, the calibration was applied to the raw data and the energy of the aforementioned ^{12}C, ^{16}O, and ^{26}Al states is compared to the literature value. The difference between the measured energy and the tabulated one was minimized by repeating the procedure for several ($E_{\rm beam}$, θ_{SP}) setting pairs. The best result was obtained for $E_{\rm beam} = 18.001$ MeV $\pm$ 3 keV and $\theta_{SP} = 40.2° \pm 0.2°$, in very good agreement with the magnetic field value of the Tandem analyzing magnet and the Split-Pole angular positioning system, respectively. The calibration residuals are at maximum 2 keV. Proton and deuteron energy losses in the target were taken into account. Reactions were assumed to take place in the middle of the target, which is justified for thin targets. The focal-plane calibration obtained in these conditions was used for all other magnetic field settings.

While proton peaks at low excitation energies are well isolated and can be unambiguously associated to ^{27}Al states, the situation is more complicated at higher excitation energies where (*i*) the level density is much higher leading to overlapping levels, (*ii*) the background is more significant, and (*iii*) there is very limited spectroscopic information on ^{27}Al in this energy range. Hence the origin of a given proton peak cannot be *a priori* assumed to be ^{27}Al. To infer the proton peak origin the mass kinematic displacement was determined by comparing the protons focal-plane spectra obtained at spectrometer angles of 40° and 45°. At each angle a magnetic rigidity list for the proton peaks across the whole focal plane has been established using an automatic peak search routine. Taking the 40° magnetic rigidity list as a reference, the 45° list was shifted by steps of 2 keV and the number of coincidence peaks within a matching window of 4 keV was plotted as a function of the rigidity shift (see Fig. 3). A clear peak corresponding to the experimental kinematic displacement was observed on top of a random peak association background. Calculation of the kinematic displacement associated to the ^{27}Al$(p,p')^{27}$Al* reaction for an excited state at 13 MeV (middle of the focal plane) is also shown (dashed line). The very good agreement between the measured and calculated kinematic displacement indicates that the observed proton peaks correspond to ^{27}Al states with high

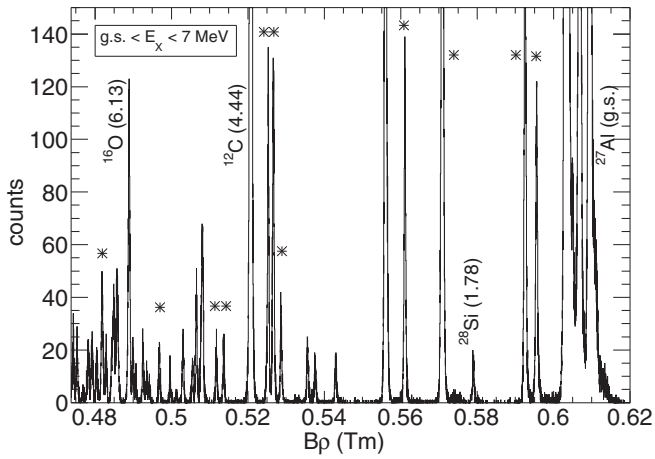

FIG. 2. Proton rigidity spectrum used for focal-plane position calibration. Excitation energies up to about 7 MeV are covered, including ground states above 0.6 T m. All proton peaks correspond to known ^{27}Al states unless this is indicated. ^{27}Al states labeled with an asterisk have been used for the focal-plane calibration (see text).

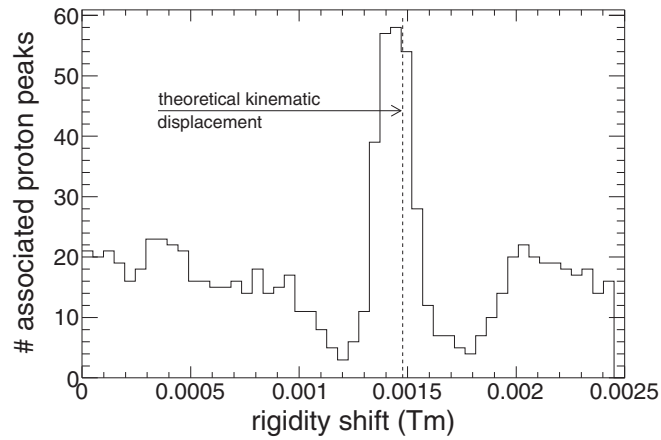

FIG. 3. Number of associated proton peaks between focal-plane position spectra at spectrometer angles of 40° and 45° as a function of rigidity shift (see text for details). The dashed vertical line corresponds to the calculated kinematic displacement for the ^{27}Al$(p,p')^{27}$Al* reaction for a state in the middle of the focal plane.

confidence. It also indicates that proton peaks associated to the same levels are present at these two angles. The limited number of observed contaminant proton peaks does not affect the above conclusions.

B. States below the ^{23}Na + α threshold

There are 160 ^{27}Al excited states reported in the literature [29] below the ^{23}Na + α threshold [$S_\alpha = 10091.8(1)$ keV]. All known isolated states are observed in the present experiment. Even in case of nearby states which cannot be experimentally resolved, proton peaks are always observed in the present data. These observations corroborate previous proton inelastic scattering measurements off ^{27}Al [25,26] where most of the ^{27}Al states up to the ^{23}Na + α threshold were populated. These data also confirm the very small selectivity of the ^{27}Al$(p,p')^{27}$Al* reaction. Indeed the seven states with known spins greater than 7/2 (corresponding to possible spin values for s- and p-wave neutron capture on ^{26}Al) are populated with a similar strength as states with lower spins. It is worth noting that these data show no indication of additional states below the ^{23}Na + α threshold.

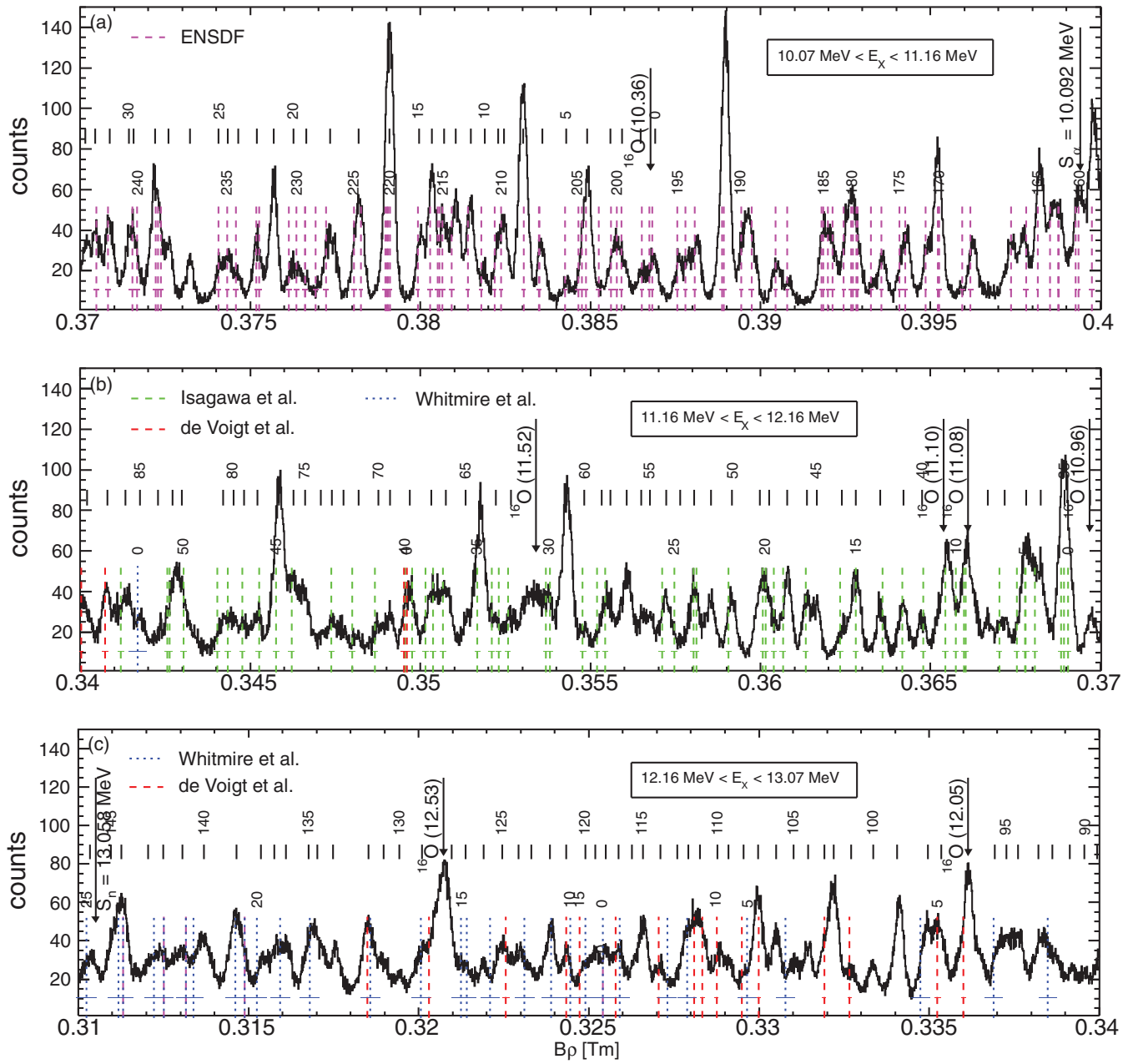

FIG. 4. (Color online) Proton magnetic rigidity spectrum at spectrometer angle of 40°. Excitation energies between the alpha and neutron thresholds in ^{27}Al are presented. The upper vertical lines with associated numbers refer to ^{27}Al states observed in the present work. The lower vertical dashed lines and numbers refer to known states from ENSDF [29] and Isagawa *et al.* [30], Whitmire *et al.* [23], and de Voigt *et al.* [31] works as indicated in each panel. The horizontal bars represents the energy uncertainty for known states. Oxygen contamination lines are also indicated.

C. States above the ^{23}Na + α threshold

Proton focal-plane spectra obtained with the ^{27}Al target at a spectrometer angle of 40° are shown in Fig. 4. These spectra cover excitation energies between the alpha emission and neutron emission thresholds, i.e., between 10.07 and 13.07 MeV. Carbon excited states in this energy range have a large natural width ($\Gamma > 250$ keV) and are weakly populated so they did not produce any observed contaminant lines. Concerning oxygen induced contamination, the states at 10.36, 10.96, 11.08, 11.10, 12.05, and 12.53 MeV as well as the broad state at 11.52 MeV ($\Gamma = 71$ keV) are populated as has been observed with the mylar target. Known ^{27}Al states reported in ENSDF [29] ($E_X \leqslant 11.188$ MeV) are represented as vertical lines in Fig. 4 (top). All known states could be associated to proton peaks in our data. Some proton peaks are observed for the first time, e.g., between states 231 and 232 as well as between states 236 and 237, and do not correspond to any carbon nor oxygen lines. Above excitation energies of 11.188 MeV, ^{27}Al states have been previously populated by means of the ^{26}Mg + p reaction [30] and the ^{23}Na + α reaction [23,31]. In their work Isagawa *et al.* [30] reported 54 levels up to an excitation energy of 12.118 MeV. These states are represented by vertical dashed lines in Fig. 4 (middle) and a very good agreement is observed with our data. At higher excitation energies (Fig. 4, bottom) while all states observed in the ^{23}Na(α,γ)^{27}Al measurement [31] can be associated to proton peaks in our data, states populated by the ^{23}Na($\alpha,p_{0,1}$)^{26}Mg reaction [23] are difficult to associate to proton peaks in our data. No better agreement could be obtained by changing all state energies within the large reported associated uncertainty (≈10 keV).

A fit of the proton spectrum has been performed and a list of new ^{27}Al states with their energies are given in Table I. In total 30 new states are observed. The smoothly increasing background observed in Fig. 4 was modeled by a one-degree polynomial which was subtracted to the data before fitting. Since most of the levels reported in ENSDF [29] have a natural width much smaller than the experimental width, a common width was taken for each Gaussian function describing ^{27}Al states in the fitting procedure. The width (≈12 keV FWHM) is determined from well isolated ^{27}Al levels (e.g., states 187, 188, or 213) and reflects the experimental resolution in this energy range. Neglecting possible natural widths may thus lead to the identification of several states while only one broad state could be present. As an example a symmetric broad proton peaks could be interpreted as two equally populated states (see Table I).

D. States above the ^{26}Al + n threshold

Proton focal-plane spectra obtained with the ^{27}Al target are shown in Fig. 5 for spectrometer angles of 10° (upper panel) and 40° (lower panel). The spectra cover an energy region about 700 keV above the ^{26}Al + n threshold [S_n = 13057.91(12) keV]. Proton focal-plane spectra obtained at 40° with the carbon and mylar targets are also shown in Fig. 5 (lower panel, bottom). The main proton peak comes from the strongly populated 12.710(6) MeV ^{12}C state which is indeed observed in the ^{27}Al proton spectra. Contaminant lines from ^{16}O states are present but weakly populated. The shift in position of the 12.71 MeV ^{12}C state as observed with the carbon and mylar targets comes from the different proton energy losses in the targets and the different beam optics when running at low beam intensity on the mylar target.

A fit of the proton spectrum after linear background subtraction is superimposed to the data obtained at 40° (Fig. 5 lower panel, middle). This was achieved by performing a least-squares fit of multiple Gaussian functions. A common peak width (FWHM) of about ≈12 keV was obtained. This is the same as obtained from the analysis of the isolated 12.71 MeV ^{12}C state during a dedicated ^{12}C target run where the focal-plane detector position was adjusted to the ^{12}C(p,p')^{12}C$^*_{12.71}$ reaction. The proton peak associated to the

TABLE I. ^{27}Al states between the alpha and neutron threshold energy deduced from the present data. Excitation energies are given in keV and accurate within 4 keV.

No.	E_X	No.	E_X	No.	E_X	No.	E_X	No.	E_X	No.	E_X	No.	E_X	No.	E_X	No.	E_X	No.	E_X
0	10560	15	10810	30	11112[a]	45	11446	60	11676	75	11946	90	12176	105	12445	120	12633	135	12877
	10575		10841		11132		11456		11693		11957		12190		12461		12650		12897[a]
	10595		10874		11147		11475		11747		11971		12206		12477		12665		12907[a]
	10607		10903		11157		11493[a]		11762		11992		12219		12490		12681		12918
	10632		10928		11173		11502[a]		11777		12005		12238		12504		12693		12940
5	10654	20	10942	35	11195	50	11530	65	11791	80	12014	95	12249	110	12514	125	12707	140	12968
	10680		10962		11219		11551		11811		12024		12260		12530		12724		12986
	10700		10980		11234		11568		11825		12064[a]		12309		12541		12740		13003
	10721		11000		11256		11582		11846		12073[a]		12322		12551		12752		13016
	10726		11010		11273		11595		11865		12086		12350		12566		12778		13037
10	10741	25	11020	40	11340	55	11611[a]	70	11876	85	12103	100	12372	115	12582	130	12798	145	13047
	10756		11049		11359		11620[a]		11895		12117		12392		12591		12812		
	10771		11072		11382		11634		11910[a]		12134		12409		12603		12825		
	10784		11085		11406		11650		11920[a]		12153[a]		12417		12614		12856		
	10797		11108[a]		11421		11659		11931[a]		12164[a]		12432		12624		12870		

[a]Could also be a broad unique state.

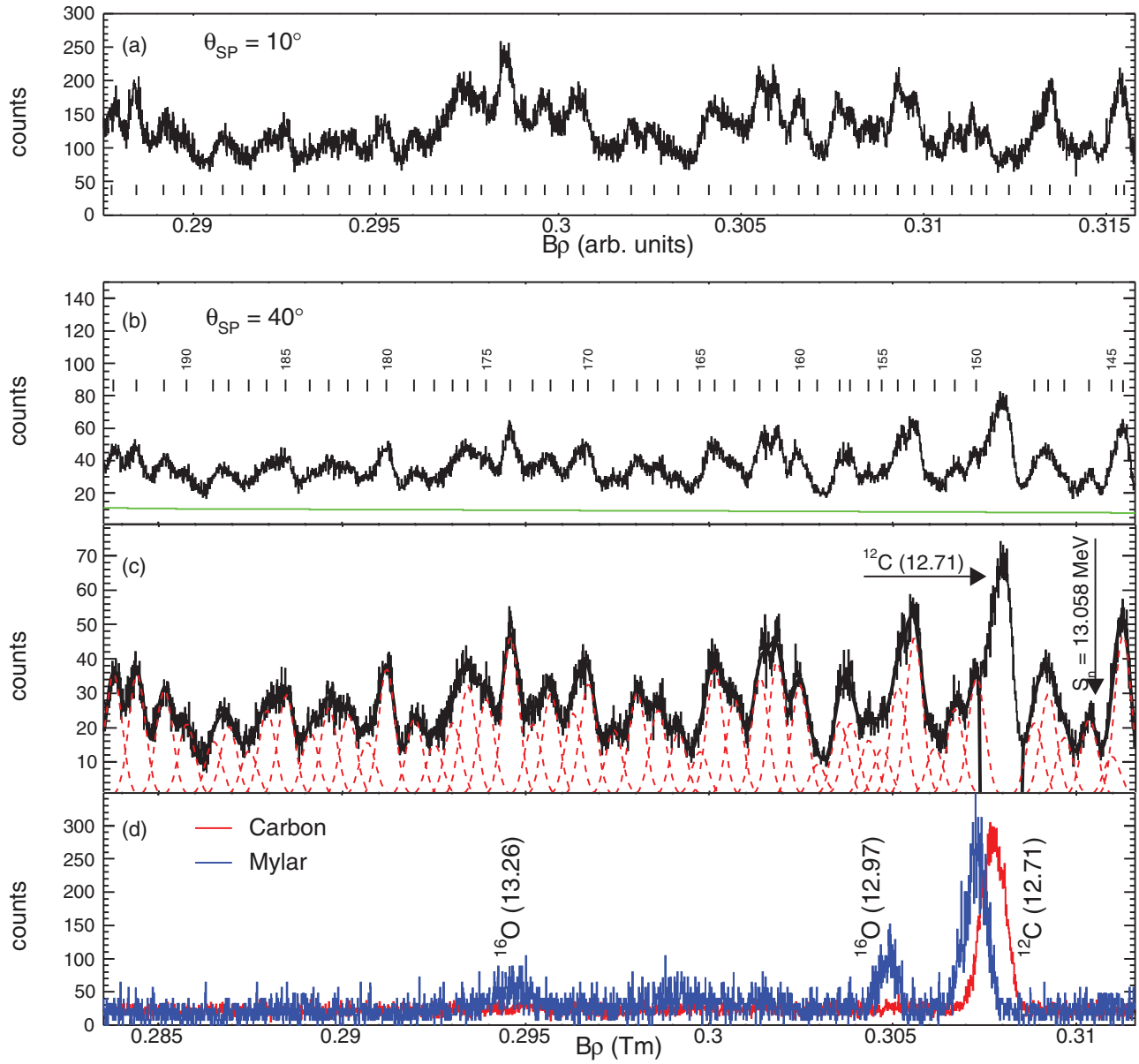

FIG. 5. (Color online) *Upper panel:* Proton magnetic rigidity spectrum at spectrometer angle of 10°. Excitation energies within about 720 keV above the ^{26}Al + n threshold are covered. *Lower panel (top):* Same as upper panel but for a spectrometer angle of 40°. The upper vertical lines with associated numbers refer to ^{27}Al states observed in the present work. *Lower panel (middle):* Fit of proton spectrum after background subtraction. The subtracted background is represented by a straight line in the lower panel (top). *Lower panel (bottom):* Spectra obtained with the carbon (80 μg/cm^2) and mylar (203 μg/cm^2) targets showing the contaminant peaks in the region of interest.

12.71 MeV state was adequately described by a Gaussian shape function. In the ^{27}Al data the energy region around the ^{12}C contaminant line was not included in the fitting procedure at 40°. However, ^{27}Al states in this region were observed in the data at 10° since the carbon peak has moved away to another position in the focal plane at this angle. Excitation energies were extracted with an uncertainty of 4 keV. Results were stable when varying by ±20% the amount of background subtracted, except for the weakly populated states for which an additional uncertainty of 1 keV is added on their energies. The same fitting procedure has been applied to the data at 10° and magnetic rigidities have been extracted for all populated levels. Most of the levels are observed at both angles and the statistical distribution of the level energy difference has a RMS of 6 keV for 93% of the levels.

Excitation energies deduced from this work are listed in Table II together with results from previous studies. More than 30 new ^{27}Al states above the neutron threshold are observed. These results are in excellent agreement with the ^{23}Na(α,γ)^{27}Al measurement of de Voigt *et al.* [31]. However, a comparison with the ^{23}Na($\alpha, p_{0,1}$)^{26}Mg measurements of Whitmire *et al.* [23] is more difficult due to the large uncertainties in their energy determination. Recently, neutron resonances have been populated using the ^{26}Al(n,α)^{26}Mg

TABLE II. Levels above the neutron threshold [$S_n = 13057.91(12)$ keV] in ^{27}Al from the present work in comparison with literature values. Excitation energies are accurate within 4 keV.

No.	E_X (keV)				
	This work	de Voigt *et al.*[a]	Whitmire *et al.*[a]		de Smet *et al.*
	(p,p')	(α,γ)	(α,p_0)	(α,p_1)	(n,α)
146	13063			13063.1 ± 8.5	13064.0 ± 0.1[b]
	13082[c]		13077.5 ± 8.5		13080.7 ± 0.1
	13095[c]				13094.2 ± 0.2
	13106[c]				13100.8 ± 0.2
	carbon contamination			13121.0 ± 8.5	
	carbon contamination		13124.4 ± 8.5		
	carbon contamination				13146.4 ± 0.8
150	13151[d]				
	13168			13158.5 ± 8.5	13170.6 ± 1.1
	13184[d]		13177.2 ± 8.5	13182.3 ± 8.5	
	13200	13198.5 ± 2.6	13202.8 ± 8.5		
	13212			13216.4 ± 8.5	
155	13225				
	13235				
	13249[c]				
	13258[c]				
	13275[c]				
160	13289	13287.9 ± 2.6			
	13306	13305.0 ± 2.6			
	13319				
	13338				
	13354	13353.5 ± 2.6			
165	13365[d]				
	13381				
	13397				
	13412				
	13430				
170	13449				
	13461				
	13478				
	13491				
	13508				
175	13526				
	13540				
	13551				
	13565[d]				
	13579				
180	13600				
	13614				
	13628				
	13643				
	13656				
185	13674				
	13688				
	13701[d]				
	13716[c]				
	13727[c]				
190	13746				
	13762				
	13782				
	13799				

[a]Levels energy given in the original works have been corrected for the actual alpha emission threshold energy [$S_\alpha = 10091.8(1)$ keV] in ^{27}Al.
[b]Uncertainty comes from the neutron threshold energy uncertainty.
[c]Could also be a broad single state.
[d]Excitation energy is accurate within 5 keV.

reaction [20], confirming the energies of neutron resonances obtained from previous direct ^{26}Al + n measurements [19] and time-reverse measurements [17,32]. All these neutron resonances were observed in the present data.

Previous reaction studies exhibit different selectivity and hence populate states with different spins and parities. The ^{26}Al + n measurements [19,20] populate high-spin states, e.g., $J^\pi = \{9/2^+, 11/2^+\}$ and $\{7/2^-, 9/2^-, 11/2^-, 13/2^-\}$ corresponding to s-, and p-wave neutron capture, respectively. The ^{23}Na(α,γ)^{27}Al reaction mechanism also tends to populate relatively high-spin ($J > 5/2$) states [31]. In contrast, the ^{23}Na(α,p)^{26}Mg reaction mainly populates spins lower than 7/2 [24]. Based on the existing ^{23}Na(α,γ)^{27}Al measurement we tentatively deduce that the seven new states between $13.2 < E_X(^{27}\text{Al}) < 13.4$ MeV have low spins. Nothing can be inferred for states at higher excitation energies since they are observed here for the first time.

IV. CONCLUSIONS

A high-resolution measurement of the ^{27}Al(p,p')^{27}Al* reaction has been performed and states up to excitation energies of around 14 MeV have been populated. Energies for all these states have been determined and agree well with existing measurements. 30 states above the ^{23}Na + α threshold and more than 30 states above the ^{26}Al + n threshold have been reported for the first time. For states between 13.0 and 13.4 MeV, we tentatively make a distinction between low and high spin states based on the spin and parity selectivity of previous measurements. The number of levels observed in the present work is lower than that predicted by the Hauser-Feshbach calculations which may question its validity in this case. However without robust spin and parity assignments quantitative conclusions cannot be drawn.

In the absence of direct measurements of the ^{23}Na(α,p)^{26}Mg and ^{26}Al + n reactions across the whole energy region of interest, the determination of properties of relevant ^{27}Al states is crucial to reduce the current uncertainty in these reaction rates. In this work, the level structure of ^{27}Al has been studied across the full energy range of interest for the first time, and excitation energies have been determined with a typical uncertainty of 4 keV. Further complementary measurements of the branching ratios [33], partial widths and spins and parities are required to reduce the uncertainties in the reaction rate calculations and allow a precise determination of the ^{26}Al production in massive stars. The improved knowledge of the ^{27}Al level scheme from the present work will not only guide future direct measurements, but is also important for future spectroscopic studies of relevant states.

ACKNOWLEDGMENTS

The continued support of the staff of the Tandem-Alto facility as well as the target laboratory staff is gratefully acknowledged. A.M.L. and S.P.F. acknowledge the support of the Science and Technology Facilities Council. This work has been supported by the European Community FP7 Capacities-Integrated Infrastructure Initiative, Contract ENSAR No. 262010 and the French-Spanish AIC-D-2011-0820 project. This work was (partly) supported by the Helmholtz Association (H.G.F.) through the Nuclear Astrophysics Virtual Institute (VH-VI-417).

[1] N. Prantzos and R. Diehl, Phys. Rep. **267**, 1 (1996).
[2] W. A. Mahoney, J. C. Ling, W. A. Wheaton, and A. S. Jacobson, Astrophys. J. **286**, 578 (1984).
[3] G. H. Share, R. L. Kinzer, J. D. Kurfess, D. J. Forrest, E. L. Chupp, and E. Rieger, Astrophys. J. Lett. **292**, L61 (1985).
[4] B. J. Teegarden, S. D. Barthelmy, N. Gehrels, J. Tueller, M. Leventhal, and C. J. MacCallum, Astrophys. J. Lett. **375**, L9 (1991).
[5] S. Plüschke, R. Diehl, V. Schönfelder, H. Bloemen, W. Hermsen, K. Bennett, C. Winkler, M. McConnell, J. Ryan, U. Oberlack *et al.*, in *Exploring the Gamma-Ray Universe*, edited by A. Gimenez, V. Reglero, and C. Winkler, ESA Special Publication Vol. 459 (ESA Publication Division, Noordwijk, The Netherlands, 2001), p. 55.
[6] J. Knödlseder, Astrophys. J. **510**, 915 (1999).
[7] R. Diehl, H. Halloin, K. Kretschmer, G. G. Lichti, V. Schönfelder, A. W. Strong, A. von Kienlin, W. Wang, P. Jean, J. Knödlseder *et al.*, Nature (London) **439**, 45 (2006).
[8] K. Kretschmer, R. Diehl, M. Krause, A. Burkert, K. Fierlinger, O. Gerhard, J. Greiner, and W. Wang, Astron. Astrophys. **559**, A99 (2013).
[9] T. Lee, D. A. Papanastassiou, and G. J. Wasserburg, Geophys. Res. Lett. **3**, 41 (1976).
[10] B. Jacobsen, Q.-z. Yin, F. Moynier, Y. Amelin, A. N. Krot, K. Nagashima, I. D. Hutcheon, and H. Palme, Earth Planet. Sci. Lett. **272**, 353 (2008).
[11] A. G. W. Cameron and J. W. Truran, Icarus **30**, 447 (1977).
[12] V. Tatischeff, J. Duprat, and N. de Séréville, Astrophys. J. Lett. **714**, L26 (2010).
[13] M. Limongi and A. Chieffi, Astrophys. J. **647**, 483 (2006).
[14] C. Iliadis, A. Champagne, A. Chieffi, and M. Limongi, Astrophys. J. Suppl. **193**, 16 (2011).
[15] E. Bravo and G. Martínez-Pinedo, Phys. Rev. C **85**, 055805 (2012).
[16] A. Parikh, J. José, I. R. Seitenzahl, and F. K. Röpke, Astron. Astrophys. **557**, A3 (2013).
[17] R. T. Skelton, R. W. Kavanagh, and D. G. Sargood, Phys. Rev. C **35**, 45 (1987).
[18] H. P. Trautvetter, H. W. Becker, U. Heinemann, L. Buchmann, C. Rolfs, F. Käppeler, M. Baumann, H. Freiesleben, H.-J. Lütke-Stetzkamp, P. Geltenbort *et al.*, Z. Phys. A **323**, 1 (1986).
[19] P. E. Koehler, R. W. Kavanagh, R. B. Vogelaar, Y. M. Gledenov, and Y. P. Popov, Phys. Rev. C **56**, 1138 (1997).
[20] L. de Smet, C. Wagemans, J. Wagemans, J. Heyse, and J. van Gils, Phys. Rev. C **76**, 045804 (2007).
[21] B. M. Oginni, C. Iliadis, and A. E. Champagne, Phys. Rev. C **83**, 025802 (2011).
[22] T. Rauscher and F.-K. Thielemann, At. Data Nucl. Data Tables **75**, 1 (2000).
[23] D. P. Whitmire and C. N. Davids, Phys. Rev. C **9**, 996 (1974).
[24] J. Kuperus, Physica **30**, 2253 (1964).

[25] C. Doekes, D. Kean, F. Elliott, and R. Spear, Can. J. Phys. **49**, 483 (1971).
[26] C. Moss and J. Sherman, Nucl. Phys. A **259**, 413 (1976).
[27] J. E. Spencer and H. A. Enge, Nucl. Instrum. Methods **49**, 181 (1967).
[28] R. G. Markham and R. G. Robertson, Nucl. Instrum. Methods **129**, 131 (1975).
[29] M. Shamsuzzoha Basunia, Nucl. Data Sheets **112**, 1875 (2011).
[30] K. Isagawa, K. Nakayama, and Y. Oda, J. Phys. Soc. Jpn. **48**, 1804 (1980).
[31] M. De Voigt, J. Maas, D. Veenhof, and C. Van Der Leun, Nucl. Phys. A **170**, 449 (1971).
[32] G. Doukellis and J. Rapaport, Nucl. Phys. A **467**, 511 (1987).
[33] S. Benamara, N. de Séréville, P. Adsley, A. M. Laird *et al.*, in Proceedings for Nuclear Physics in Astrophysics VI, Lisbon, 2013 [J. Phys.: Conf. Ser. (to be published)].